Published in final edited form as:
Methods Mol Biol. 2007 ; 374: 147–159.

Sentinel Lymph Node Mapping with Type II Quantum Dots

John V. Frangioni, M.D., Ph.D.[*], **Sang-Wook Kim, Ph.D.**[†], **Shunsuke Ohnishi, M.D., Ph.D.**[*], **Sungjee Kim, Ph.D.**, and **Moungi G. Bawendi, Ph.D.**[†]

[*]*Division of Hematology/Oncology and Department of Radiology, Beth Israel Deaconess Medical Center, Harvard Medical School, Boston, MA 02215*

[†]*Department of Chemistry, Massachusetts Institute of Technology, Cambridge, MA 02139*

Abstract

Sentinel lymph node (SLN) mapping is an important cancer surgery during which the first lymph node draining the site of a tumor is identified, resected, and analyzed for the presence or absence of malignant cells. Fluorescent semiconductor nanocrystals (quantum dots) of the appropriate size, charge, and emission wavelength permit this surgery to be performed rapidly, with high sensitivity, and under complete image guidance. We describe the materials and methods necessary for the production and characterization of type II near-infrared (NIR) fluorescent quantum dots, which have been optimized for SLN mapping. They contain a CdTe core, CdSe shell, and highly anionic, oligomeric phosphine organic coating. We also describe how to utilize such quantum dots in animal model systems of SLN mapping.

Keywords

Quantum Dots; Near-Infrared Fluorescence; Near-Infrared Fluorescence Imaging; Imaging; Intraoperative Imaging; Sentinel Lymph Nodes

1. Introduction

In the 1990s, Morton et al., introduced the concept of sentinel lymph node (SLN) mapping and biopsy, which revolutionized the assessment of nodal status in melanoma and breast cancer [1]. The underlying hypothesis of SLN mapping is that the first lymph node to receive lymphatic drainage from a tumor site will contain tumor cells if there has been direct lymphatic spread [2]. Patients in whom SLN sampling does not reveal the presence of tumor are spared the morbidity of radical lymph node dissection.

Current techniques for SLN mapping involve preoperative injection of a radioactive colloid tracer (e.g., technetium-99m sulfur colloid) followed by intraoperative injection of a visible blue dye (e.g., isosulfan blue). The dye permits limited visualization of afferent lymphatic vessels and the SLN, while the radioactive colloid tracer improves detection rate and confirms complete harvest of the SLN with the use of an intraoperative handheld gamma probe [3]. The learning curve associated with conventional SLN mapping is steep [4], the technique itself requires ionizing radiation, and the blue dye is extremely difficult to find in the presence of blood and anthracosis.

Corresponding Author: Moungi G. Bawendi, Ph.D., MIT 6-221, 77 Massachusetts Avenue, Cambridge, MA 02139-4307, Phone: 617-253-9796, FAX: 617-253-7030, Email: mgb@mit.edu.

There are three important parameters in designing a lymphatic tracer for SLN mapping: hydrodynamic diameter (HD), surface charge, and contrast generation. Molecules with a HD less than approximately 10 nm have the potential to travel beyond the SLN. For very small agents, such as isosulfan blue, this can result in missing the SLN, but more likely, will result in more than one nodal group in the same chain being labeled. Very large molecules, in the range of 50–100 nm have difficulty even entering lymphatic channels, and travel so slowly that up to 24 hours may be required to label the SLN (reviewed in [5]). With respect to surface charge, anionic molecules have rapid uptake into lymphatics and excellent retention in lymph nodes [6]. With respect to contrast generation, agents presently being used clinically are either radioactive gamma emitters or colored dyes.

In 2004, our group introduced near-infrared (NIR) fluorescent quantum dots (QDs) for SLN mapping and resection. NIR light, otherwise invisible to the human eye, provides extremely high signal to background ratios (SBRs) without changing the look of the surgical field. A thorough discussion of the use of NIR light in biomedical imaging has been published previously [7]. When combined with a suitable intraoperative imaging system [8,9], the advantage of NIR quantum dots for SLN mapping include high sensitivity, real-time and simultaneous visualization of both surgical anatomy and lymphatic flow, and non-radioactive detection. In this manuscript, we describe in detail the production and use of type II NIR fluorescent quantum dots for SLN mapping and resection. These NIR QDs have been specifically engineered with a HD (15–20 nm) that permits rapid uptake into lymphatic channels but ensures retention in the SLN, a highly anionic surface charge, maximal absorption cross-section, and a suitable quantum yield.

2. Materials

2.1 Quantum Dot Chemicals

Trioctylphosphine oxide (TOPO, Alfa Aeser, Ward Hill, MA), cadmium acetylactonate (Cd $(acac)_2$; Alfa Aeser), hexadecylamine (90%; Aldrich, St. Louis, MO), tri-n-octylphosphine (TOP; 97%; Strem, Newburyport, MA), tellurium shot (99.999%; Alfa Aeser), bis-(trimethylsilyl)selenide (98%; Acros Organics, Geel, Belgium), trishydroxypropylphosphine (90; Strem), diisocyanatohexane (98%; Aldrich) and ethyl isocynatoacetate (95%; Aldrich) were used as supplied. Dimethylcadium (Strem; 99%) was filtered to remove impurities using a 0.2 μm syringe filter (Pall Corporation, East Hills, NY). A tellurium stock solution (0.5 M) was prepared by dissolving 3.2 g of tellurium shot in 50 ml of TOP at room temperature, stirring gently for a few hours, yielding a yellow solution.

2.2 Gel-Filtration Chromatography and Optical Measurements

The gel-filtration chromatography system consisted of an ÄKTA prime pump with fraction collector, and Superose-6 10/300 GL gel-filtration column (Amersham Biosciences, Piscataway, NJ). On-line absorbance spectrometry was performed with a model 75.3-Q-10, 1-cm path length, 70 μL quartz flow cell (Starna, Atascadero, CA), USB2000 fiber optic spectrometer and CHEM2000-UV-VIS light source with cuvette holder (Ocean Optics, Dunedin, FL). On-line fluorescence spectrometry was performed with a model 583.4.2F-Q-10, 1-cm path length, 80 μL flow cell (Starna), HR2000 fiber optic spectrometer and CUV-ALL-UV 4-way cuvette holder (Ocean Optics), and the desired laser diode set to 5 mW with output coupled through a 300 μm core diameter, NA 0.22 fiber (Fiberguide Industries, Stirling, NJ). Laser diodes used with the system include 5W 532 nm, 5W 670 nm, or 250 mW 770 nm (Electro Optical Components, Santa Rosa, CA). Data acquisition was performed with two Dell computers using the OOIBase32 spectrometer operating software package (Ocean Optics). The spectral range of USB2000 spectrometer was from 200 nm to 870 nm with a spectral resolution

of 1 nm, and that of HR2000 spectrometer was from 200 nm to 1100 nm with a spectral resolution of 6.7 nm.

2.3 Animal Models

Animals were housed in an AAALAC-certified facility staffed by full-time veterinarians, and were studied under the supervision of an approved institutional protocol. This protocol adhered to the "NIH Principles for the Utilization and Care of Vertebrate Animals Used in Testing, Research, and Training." Sprague-Dawley rats were purchased from Taconic Farms (Germantown, NY) at 300–350 g size and were of either sex. Yorkshire pigs were typically female to permit SLN mapping of mammary tissue and were purchased at 35 kg from E.M. Parsons and Sons (Hadley, MA). All animals acclimated to the animal facility for at least 48 hours prior to experimentation. After each study, anesthetized rats were euthanized by intra-peritoneal injection of 200 mg/kg pentobarbital, and anesthetized pigs were euthanized by rapid intravenous injection of 10 ml of Fatal-Plus (Vortech Pharmaceuticals, Dearborn, MI). These methods of euthanasia are consistent with the recommendations of the Panel on Euthanasia of the American Veterinary Medical Association.

3. Methods

3.1 Preparation of Near-Infrared Fluorescent Type II Quantum Dots

Conventional type I core-shell fluorescent semiconductor nanocrystals (quantum dots; QDs) confine both electrons and holes in the core. The band offsets between the core and the shell are engineered such that the conduction band of the outer band gap material is of higher energy than that of the inner band gap material, and the valence band of the outer band gap material is of lower energy than that of the inner band gap material. Quantum confinement effects in the core semiconductor determine the range of energies possible for fluorescence in these type I structures (Figure 1A). The purpose of the shell is to provide a protective barrier that enhances the chemical stability and the quantum efficiency. In CdTe(CdSe) core(shell) QDs, the offset structure of the band implies that electrons and holes are to some extent spatially separated between the core and shell, with the holes mostly confined to the core and the electrons having a preference for the shell (Figure 1A). The emission energy in these type II structures then depends on the band offsets of the core and shell materials. Type II QDs can therefore emit at energies smaller than either band gap of the composite materials. Both the thickness of the shell and the diameter of the core control the effective band gap of these QDs. This feature provides a new degree of flexibility in designing and engineering QD structures by largely removing the traditional correlation between QD size and its emission wavelength. This has allowed us to tailor QDs to have a size and emission wavelength specifically optimized for SLN mapping.

3.1.1 Synthesis of the Core—TOPO (6.25 g), hexadecylamine (5.75 g), and 4 ml of TOP were dried and degassed in the reaction vessel by heating to 140° C at ~1 Torr for 1 hr and flushing periodically with argon. CdTe stock solution was prepared as followed. 634 mg (2.0 mmol) of $Cd(acac)_2$ was added to 6 ml of TOP and degassed at 140° C, ~1 Torr for 1 hr. 4 ml of 0.5 M TOP-Te stock solution was added, mixed well, and cooled to room temperature. This solution was injected by syringe through a rubber septum at 350° C, producing a deep red solution. The heat was then removed from the reaction vessel and the reaction left to cool to room temperature.

3.1.2. Shell Growth—CdTe QDs are precipitated from the growth solution by adding four milliliters of butanol and enough methanol to cause precipitation (~10–30 milliliters). Precipitated CdTe QDs (~ 400 mg) are collected after centrifugation (3,000–6,000 rpm for a few minutes), dispersed in 20 g of TOPO and 10 ml of TOP, and dried under vacuum at 160°

C for 2 hours. A stock solution for over-coating is prepared by mixing a 1:1 molar ratio of dimethylcadmium and bis-(trimethylsilyl)selenide in 4 mL of TOP. The amounts of precursors are calculated based on the desired shell thickness assuming epitaxial growth. While the CdTe core solution is vigorously stirred, the previously prepared over-coating stock solution is added drop wise at 100 °C for 2 hrs and heated to 200° C. Time and reaction temperatures vary depending on the size of CdTe QDs that is over-coated. A higher temperature is necessary to overcoat the larger CdTe QDs. The growth of the CdSe shell induces the peak red-shift of photoluminescence over time (Figure 1B).

3.1.3 Oligomeric Phosphine Organic Coating—We utilize oligomeric phosphine ligands [10] to render the QDs stable in water (Figure 1C). Ligands were prepared as follows. 8.0 g of trishydroxypropylphosphine was dissolved in 20.0 g of dimethylformamide (DMF) and 4.54 g of diisocyanatohexane was added drop wise while the solution is stirred vigorously. The reaction solution is stirred at room temperature for a day after the addition. Ethyl isocynatoacetate (EIA) (19.4 g) was added drop wise and stirred overnight. Solvent and excess EIA were removed at 100 °C *in vacuo*.

For cap-exchange, 100 mg of precipitated QDs were mixed with 3.0 g oligomeric phosphine ligands in 10 ml of tetrahydrofuran (THF) and 2 ml of DMF, stirred at room temperature for 1 hr, then THF and DMF removed at 100° C *in vacuo*. The resultant viscous mixture was incubated at 120° C for 3 hrs then cooled to room temperature. 50 ml of 1 N NaOH was added, forming a two-phase suspension, and the solution was stirred vigorously at room temperature until only a single, slightly turbid dark brown solution was present. The solution was filtered through a 0.2 μM PTFE filter (Nalgene) then ultra-filtered with 1000 volumes of phosphate buffer saline, pH 7.0 using a 50 kDa cutoff membrane (Millipore).

3.2. *In Vitro* Characterization of Physical and Optical Properties

All quantum dots used in animals undergo rigorous characterization with respect to their physical and optical properties. This analysis includes the following:

3.2.1. Transmission Electron Microscopy (TEM)—TEM was performed on a JEOL model 2010 electron microscope operated at 200 kV. TEM of water dispersed type II QDs prepared as described above showed nearly spherical core/shell dots approximately 10 nm in diameter [11].

3.2.2 Estimation of QD Concentration—To obtain the extinction coefficient of NIR QDs, the total mass per QD particle was calculated by dividing the inorganic mass per particle, as measured by TEM, by the mass of inorganic cores in a dried QD sample, as measured using a Seiko model 320 thermogravimetric analyzer. The measured concentration in most cases was 1–10 μM The concentration of QDs in solution was then obtained by Beer's law after measurement of absorption using a model HP-8453 spectrometer (Hewlett-Packard).

3.2.3 Gel-Filtration Chromatography and Optical Measurements—The gel-filtration chromatography system is shown in Figure 2. Typically, 100 μl of NIR QDs at a concentration of 4 μM in phosphate buffered saline (PBS), pH 7.8 are loaded into the injector and run at a flow rate of 1 ml/min with PBS, pH 7.8 as mobile phase. On-line, full spectrum analysis of absorbance and fluorescence permits collection of desired fractions. Calibration of HD was performed by injecting 100 μL of a size standard solution containing 3.8 mg/ml blue dextran (HD = 29.5 nm), 8.8 mg/ml thyroglobulin (18.8 nm), 3.8 mg/ml alcohol dehydrogenase (10.1 nm), 6.3 mg/ml ovalbumin (6.12 nm) and 2.5 mg/ml lysozyme (3.86 nm). All size standards were purchased from (Sigma, St. Louis, MO). NIR QDs eluted from the column were

concentrated using 10,000 MW cutoff Vivaspin (Vivascience, Edgewood, NY) concentrator with a polyethersulfone membrane.

This system permits real-time analysis of QD fractions and greatly simplifies the purification of QD preparations with particular optical and physical properties. For example, Figure 3 shows the analysis of a crude NIR QD preparation with two principle populations: one eluting at 54.13 min with a HD of 17.4 nm and another eluting at 60.27 min with a HD of 13.1 nm. As suspected from the color of the peaks on the column (Figure 3B), the absorbance and fluorescence of these populations were significantly different (Figure 3C), and each peak could be collected separately for further *in vitro* and *in vivo* analysis.

3.2.4. Chemical and Photostability in Warm Plasma—To be useful for *in vivo* imaging, the purified NIR QD preparation must exhibit excellent chemical and photostability in warm plasma. As part of quality control for all NIR QD preparations, we measure fluorescence emission over time in warm bodily fluids [11]. Calf serum is used in lieu of plasma since it is more readily available, inexpensive, and has a similar protein concentration as plasma. All experiments are performed at 37°C. We specifically ensure that micro-aggregation is not occurring by filtering all samples through a 0.2 μm syringe filter and comparing fluorescence emission pre- and post-filtration. A typical NIR QD preparation will maintain ≥ 90% of NIR fluorescence emission, without micro-aggregation, after 30 min in 37°C calf serum.

3.3 Sentinel Lymph Node Mapping in Animal Model Systems

3.3.1. Animal Anesthesia—For surgery, rats were anesthetized with 75 mg/kg intraperitoneal pentobarbital. Pig anesthesia was induced with 4.4 mg/kg intramuscular Telazol (Fort Dodge Labs, Fort Dodge, IA) and anesthesia maintained through a 7 mm endotracheal tube with 1.5% isoflurane/98.5% O_2 at 5 L/min.

3.3.1. Intraoperative NIR Fluorescence Imaging Systems—Intraoperative NIR fluorescence imaging systems optimized for small animal surgery [8] and large animal surgery [9] have been described in detail previously. Briefly, they are composed of two wavelength-isolated excitation sources, one generating 0.5 mW/cm^2 400–700 nm “white” light, and the other generating 5 mW/cm^2 (large animal) to 50 mW/cm^2 (small animal) 725–775 nm light over a 8 cm (small animal) or 15 cm (large animal) diameter field of view. Simultaneous photon collection of color video and NIR fluorescence images is achieved with custom-designed optics that maintain separation of the white light and near-infrared fluorescence (> 795 nm) channels. After computer-controlled (LabVIEW) camera acquisition via custom LabVIEW (National Instruments, Austin, TX) software, anatomic (white light) and functional (near-infrared fluorescent light) images can be displayed separately and merged. All images are refreshed up to 15 times per second. The entire apparatus is suspended on an articulated arm over the surgical field, thus permitting non-invasive and non-intrusive imaging. These imaging systems permit quantum dots used during SLN mapping of large animals to be detected in solid tissue up to 1 cm thick [11] and in lung up to 5 cm thick [12].

3.3.2. Quantum Dot Injection Technique—The injection technique is critical to the success of SLN mapping. Injection too shallow or too deep into tissue results in formation of a bleb, but no migration of NIR QDs from the site. Optimal technique includes keeping the needle bevel facing upwards, and the syringe at a 45° angle relative to the plane of the tissue. Direct cannulation of lymphatic channels is not necessary. For pig experiments, 100 μl of NIR QDs were loaded into a 1 cc syringe equipped with a 25 gauge, 1/2” needle. For rat experiments, 10 μl of NIR QDs were loaded into a glass Hamilton syringe equipped with a 30 gauge, 1/2” needle. After injection, gentle thumb pressing of the injection site will increase hydrostatic pressure and greatly accelerate lymphatic flow to the SLN.

3.3.3. Real-Time Sentinel Lymph Node Mapping and Image-Guided Resection—

To date, our group has utilized NIR QD technology for SLN mapping of skin [11], esophagus [13], lung [12], gastrointestinal tract (Soltesz et al., manuscript submitted), pleural space [14], and peritoneal space (Parungo et al., manuscript submitted). We now demonstrate limb mapping in the rat and mammary tissue mapping in the pig. SLN mapping of rat lower limb (Figure 4A) and pig mammary tissue (Figure 4B) are shown in Figure 4. In both cases, the small amount and low concentration of NIR QDs injected cannot be seen on the color video images. However, NIR fluorescence imaging reveals the fine detail of lymphatic flow from the injection site to the SLN. Background autofluorescence from tissue is low in this spectral region, permitting a high SBR to be achieved, even with 67 msec (15 Hz) exposure times (Figure 4).

4. Notes

4.1 To measure HD, we prefer gel-filtration chromatography to all other analysis methods since it has the most biological relevance. TEM is not appropriate, because only the metal component of the QD is visible. Quasi-elastic light scattering tends to weight the larger particles in a sample more than the smaller ones, thus biasing results. Gel-filtration chromatography provides both peak size and size distribution of a QD sample, and by employing on-line spectrometry, permits the desired fraction to be isolated in a single step. Most importantly, literature values for the biodistribution and pharmacokinetic behavior of biomolecules *in vivo* are typically derived from gel-filtration chromatography, thus permitting a direct comparison of results obtained with NIR QDs.

4.2 The selection of QD organic coating is of crucial importance. This coating is required to render the semiconductor component soluble in aqueous buffers, determines QD stability, and determines QD quantum yield in the presence of plasma proteins. It also contributes to the overall HD and controls how the particle will interact with the biologic system under study. For SLN mapping, we have purposely chosen an oligomeric phosphine coating since it renders the NIR QDs highly anionic, stable in the presence of proteins, and reasonably luminescent [11]. We also perform quality control on each sample by incubating in 37°C serum and measuring fluorescence emission, and micro-aggregation, over time.

4.3 Preservation of type II QD NIR fluorescence during histologic processing has not been evaluated systematically. For most experiments, we embed QD-containing tissue in Tissue-Tek O.C.T. compound (Sakura Finetek, Torrance, CA), freeze in liquid nitrogen, and cryo-section tissue at 6–20 μm. However, there is significant loss of fluorescence during this process, most likely from damage to the nanocrystalline lattice. This is in sharp contrast to organic heptamethine indocyanine contrast agents, which exhibit full preservation of NIR fluorescence during frozen sectioning [13,15]. Alternative fixation and processing procedures for type II QDs need to be explored.

4.4 The technology described above provides proof of principle experiments in large animal model systems approaching the size of humans. However, the potential toxicity of cadmium and telluride preclude their use in humans until appropriate toxicology and histopathology analyses have been conducted. Future studies should also be directed at developing NIR fluorescent QD formulations that minimize or eliminate heavy metals.

6. Acknowledgements

This work was supported in part by the US National Science Foundation–Materials Research Science and Engineering Center Program under grant DMR-9808941 (M.G.B.), the US Office of Naval Research (M.G.B.), the US Department of Energy (Office of Biological and Environmental Research) grant DE-FG02-01ER63188 (J.V.F.), a Proof of Principle Award from the Center for Integration of Medicine and Innovative Technology (CIMIT; JVF), and NIH grant # R21/R33 EB-000673 (J.V.F. and M.G.B.). We thank Grisel Rivera for administrative assistance.

5. References

1. Morton DL, Wen DR, Wong JH, Economou JS, Cagle LA, Storm FK, Foshag LJ, Cochran AJ. Technical details of intraoperative lymphatic mapping for early stage melanoma. Arch Surg 1992;127:392–399. [PubMed: 1558490]
2. Cabanas RM. An approach for the treatment of penile carcinoma. Cancer 1977:456–466. [PubMed: 837331]
3. Cox CE, Pendas S, Cox JM, Joseph E, Shons AR, Yeatman T, Ku NN, Lyman GH, Berman C, Haddad F, Reintgen DS. Guidelines for sentinel node biopsy and lymphatic mapping of patients with breast cancer. Ann Surg 1998:645–651. [PubMed: 9605656]discussion 651–3
4. Schirrmeister H, Kotzerke J, Vogl F, Buck A, Czech N, Koretz K, Helm G, Kreienberg R, Kuhn T. Prospective evaluation of factors influencing success rates of sentinel node biopsy in 814 breast cancer patients. Cancer Biother Radiopharm 2004;19:784–790. [PubMed: 15665628]
5. Fujii H, Kitagawa Y, Kitajima M, Kubo A. Sentinel nodes of malignancies originating in the alimentary tract. Ann Nucl Med 2004;18:1–12. [PubMed: 15072178]
6. Josephson L, Mahmood U, Wunderbaldinger P, Tang Y, Weissleder R. Pan and sentinel lymph node visualization using a near-infrared fluorescent probe. Mol Imaging 2003;2:18–23. [PubMed: 12926234]
7. Lim YT, Kim S, Nakayama A, Stott NE, Bawendi MG, Frangioni JV. Selection of quantum dot wavelengths for biomedical assays and imaging. Molecular Imaging 2003;2:50–64. [PubMed: 12926237]
8. Nakayama A, del Monte F, Hajjar RJ, Frangioni JV. Functional near-infrared fluorescence imaging for cardiac surgery and targeted gene therapy. Molecular Imaging 2002;1:365–377. [PubMed: 12940233]
9. De Grand AM, Frangioni JV. An operational near-infrared fluorescence imaging system prototype for large animal surgery. Technol Cancer Res Treat 2003;2:553–562. [PubMed: 14640766]
10. Kim S, Bawendi MG. Oligomeric ligands for luminescent and stable nanocrystal quantum dots. J Am Chem Soc 2003;125:14652–14653. [PubMed: 14640609]
11. Kim S, Lim YT, Soltesz EG, De Grand AM, Lee J, Nakayama A, Parker JA, Mihaljevic T, Laurence RG, Dor DM, Cohn LH, Bawendi MG, Frangioni JV. Near-infrared fluorescent type II quantum dots for sentinel lymph node mapping. Nat Biotechnol 2004;22:93–97. [PubMed: 14661026]
12. Soltesz EG, Kim S, Laurence RG, De Grand AM, Parungo CP, Dor DM, Cohn LH, Bawendi MG, Frangioni JV, Mihaljevic T. Intraoperative sentinel lymph node mapping of the lung using near-infrared fluorescent quantum dots. Ann Thorac Surg 2005;79:269–277. [PubMed: 15620956]
13. Parungo CP, Ohnishi S, Kim SW, Kim SJ, Laurence RG, Soltesz EG, Chen FY, Colson YL, Cohn LH, Bawendi MG, Frangioni JV. Intraoperative identification of esophageal sentinel lymph nodes using near-infrared fluorescence imaging. J Thor Cardiovasc Surg. 2004In Press
14. Parungo CP, Colson YL, Kim S, Kim S, Cohn LH, Bawendi MG, Frangioni JV. Sentinel lymph node mapping of the pleural space. Chest. 2005In Press
15. Parungo CP, Ohnishi S, De Grand AM, Laurence RG, Soltesz EG, Colson YL, Kang PM, Mihaljevic T, Cohn LH, Frangioni JV. In vivo optical imaging of pleural space drainage to lymph nodes of prognostic significance. Ann Surg Oncol 2004;11:1085–1092. [PubMed: 15545502]

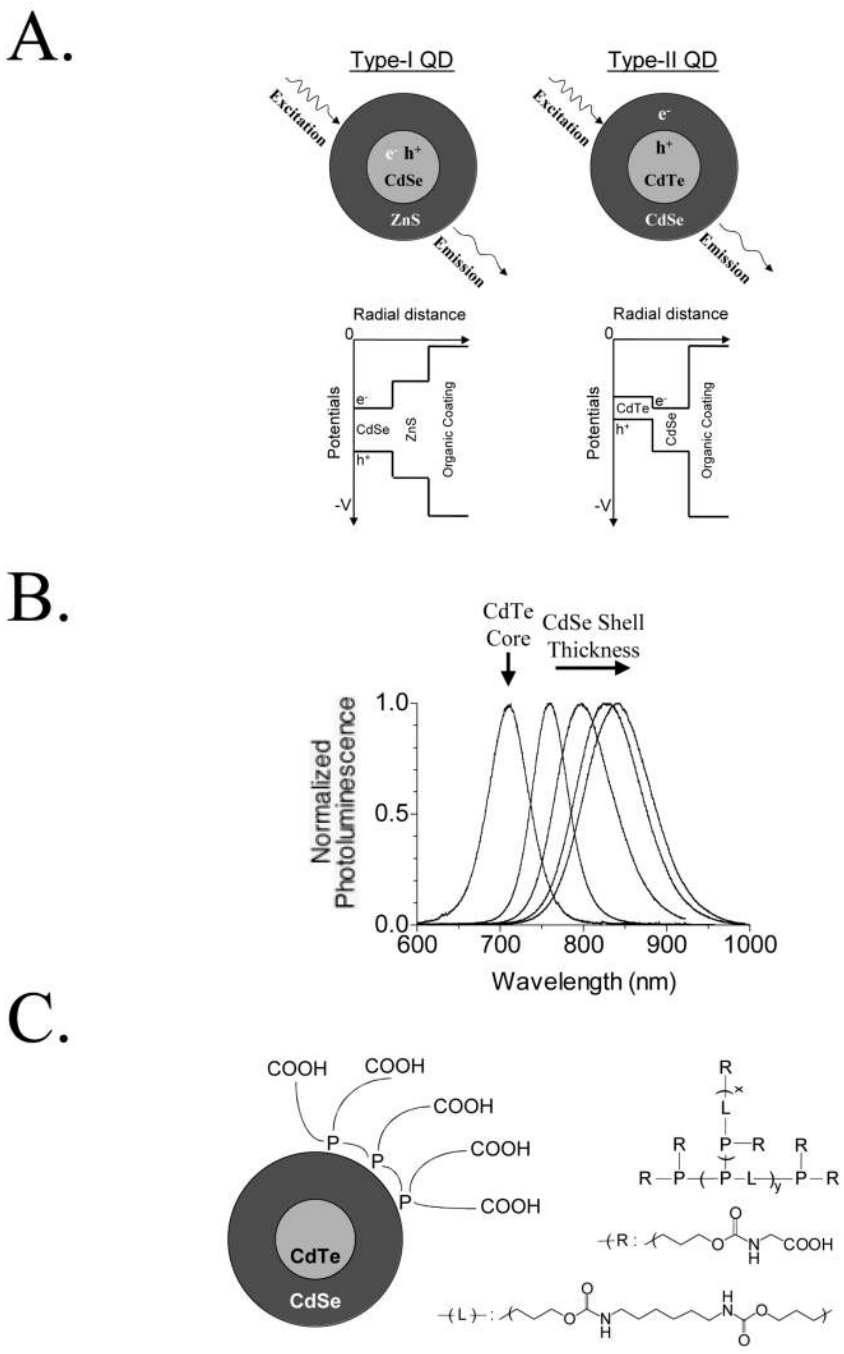

Figure 1. Type-II quantum dots and oligomeric phosphine organic coating

A. Structure of conventional type-I QDs (left) and type-II QDs (right). The chemical compositions of core and shell are shown, as are electrons (e^-) and holes (h^+). Below each structure is the potential diagram for each QD layer.

B. A CdTe core nanocrystal was coated with an increasing thickness of a CdSe shell. Shown is the change in photoluminescence over time as the type-II QD evolves towards the desired peak emission wavelength of 840–860 nm.

C. An aqueous soluble organic coating on the type-II NIR QDs described in this study is formed by cap exchange of QDs with oligomeric phosphines. The monomer, trishydroxypropyl phosphine, can form both linear and branched oligomers, can be chemically exchanged with

phosphines and phosphine oxides on the QD surface, and can be functionalized with carboxylic acids (this study) or other chemical substituents for control of surface charge and for conjugation to targeting ligands. The unit and oligomer structures are shown at right. The inner phosphine layer passivates the quantum dot surface, the hydrophobic layer protects it, and the outer layer provides functionality.

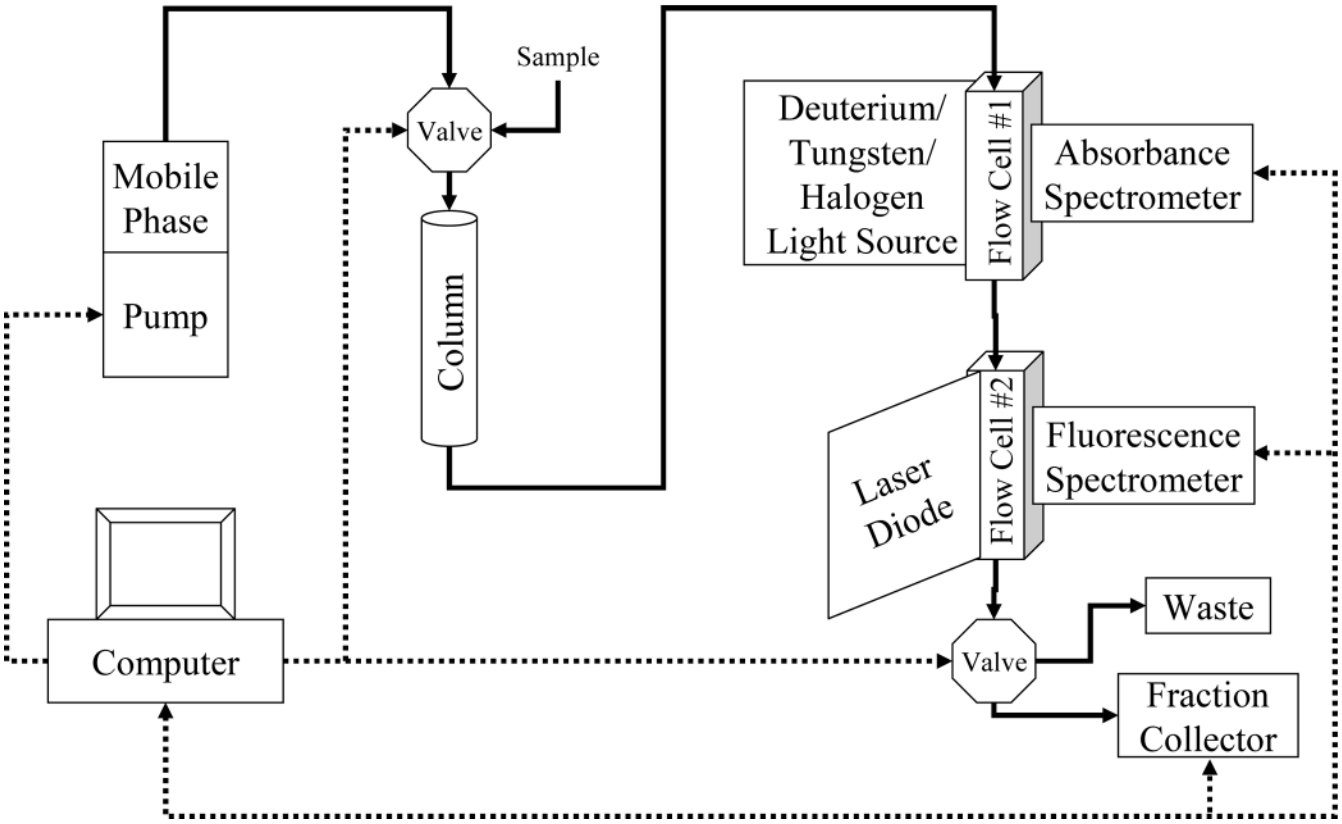

Figure 2. On-Line Full Spectrum Absorbance/Fluorescence Gel-Filtration System
Schematic diagram of the gel-filtration system components. Solid arrows denote fluid path. Dotted arrows denote computer control and data acquisition.

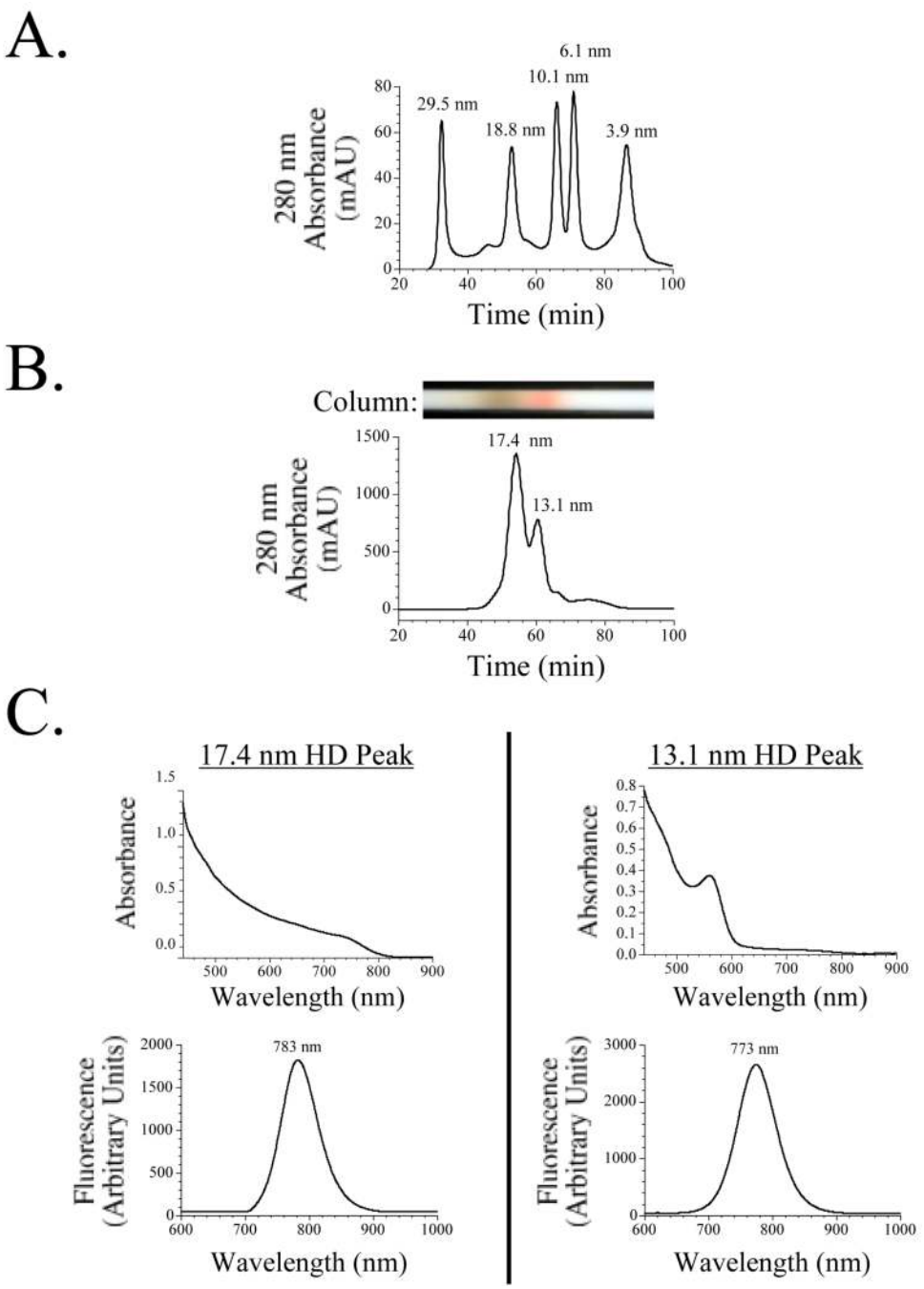

Figure 3. On-Line Analysis and Purification of NIR QD Fractions

A. For each NIR QD purification, calibration standards spanning HDs from 3.9 to 29.5 nm are detected using 280 nm absorbance (mAU).

B. The NIR QD sample is then run, with each peak calibrated in HD. Shown is the chromatogram for 280 nm absorbance (mAU). Above the chromatogram is a picture of the actual column showing the dramatic difference in color of the first (brown) and second (red) eluting peaks.

C. Real-time, full-spectrum absorbance (top panels) and fluorescence (bottom panels) for the 17.4 nm peak (left) and 13.1 nm peak (right). Fluorescence excitation was via a 532 nm laser diode.

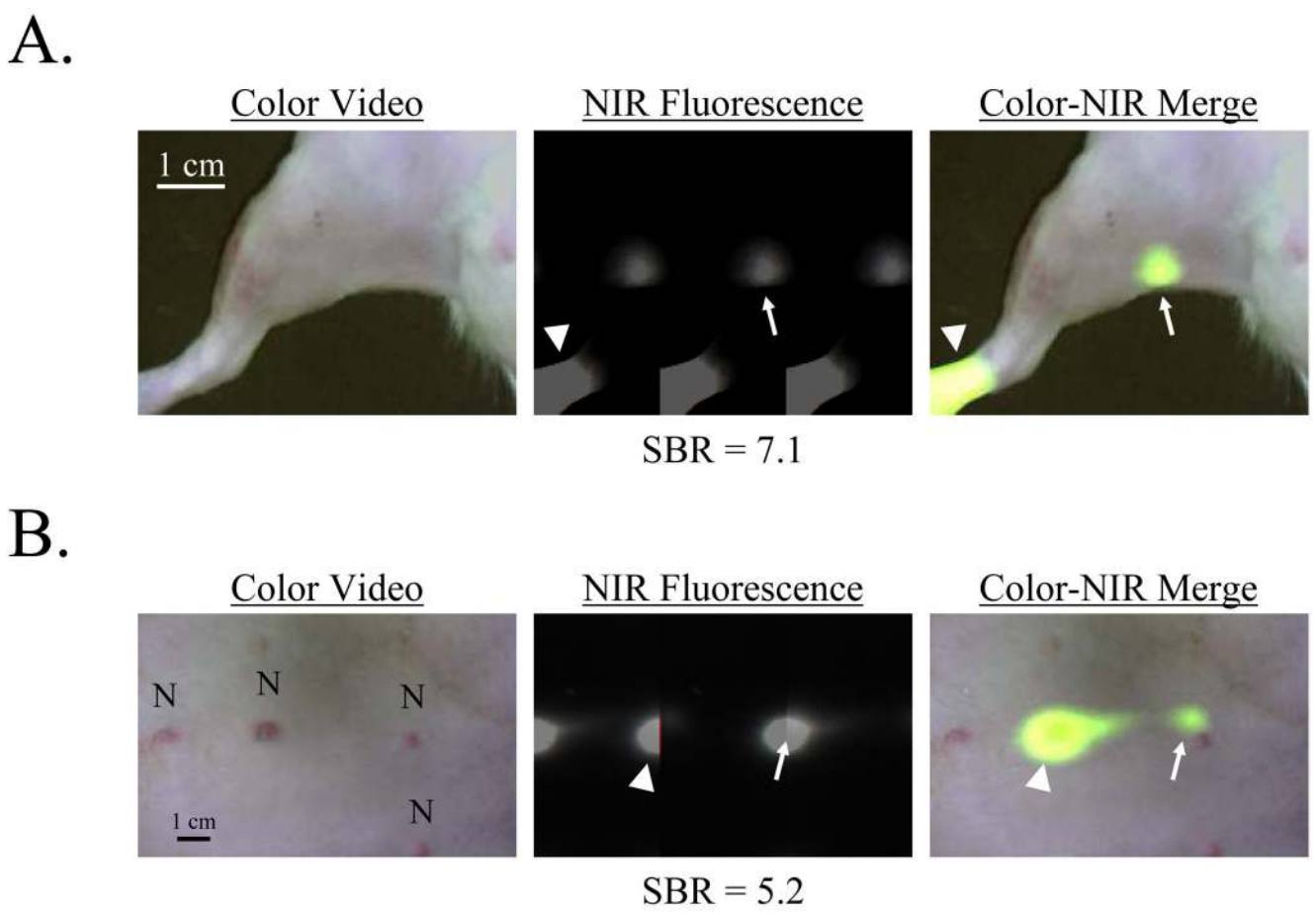

Figure 4. ***In Vivo*** **Sentinel Lymph Node Mapping in the Rat and Pig**

Type II NIR QDs were injected (arrowhead) into rat lower limb (A) or pig mammary tissue (B), and lymphatic flow mapped in real-time to the SLN (arrows). Shown are the color video image (left), the NIR fluorescence image (middle), and the pseudo-colored (lime green) merge of the two. The SBR of the SLN is shown below each NIR fluorescence image. N = nipple. NIR QD concentration was 4 μM, and injected volume was 10 μL in rat and 100 μL in pig. The fluence rate of 725–775 nm excitation light was 5 mW/cm^2 and NIR camera exposure time was 67 msec.